

# MR Imaging for Polymethylmethacralate During a Percutaneous Vertebroplasty Procedure

H. Yu<sup>1,2</sup>, R. Fahrig<sup>1</sup>, K. Butts<sup>1</sup>, A. Ganguly<sup>1</sup>, E. Adalsteinsson<sup>3,4</sup>, D. Mayer<sup>1</sup>, N. J. Pelc<sup>1</sup>

<sup>1</sup>Radiology Department, Stanford University, Stanford, CA, United States, <sup>2</sup>Electrical Engineering, Stanford University, Stanford, CA, United States, <sup>3</sup>Harvard-MIT Division of Health Sciences & Technology, Massachusetts Institute of Technology, Cambridge, MA, United States, <sup>4</sup>Department of Electrical Engineering and Computer Science, Massachusetts Institute of Technology, Cambridge, MA, United States

**Introduction** Percutaneous vertebroplasty (PV), a procedure where acrylic cement (polymethylmethacralate [PMMA]) is injected into a diseased vertebral body, has been found to provide relief from pain resulting from vertebral compression fracture [1]. The cement is made by mixing a substrate and a catalyst, and is initially in liquid form for injection, and then hardens within ~20 minutes. Image guidance during PV is usually provided by biplane fluoroscopic x-ray imaging, which offers outstanding temporal and 2D spatial resolution. However, a significant problem with viewing the PMMA is its low x-ray contrast, causing leaking cement to be difficult to observe. MR imaging of PMMA in an XMR hybrid system [2] may improve the guidance of PV. The goal of this work is to monitor the PMMA injection with MRI, by providing images that show the PMMA with high sensitivity compared to other tissues.

**Method** We collected the proton PMMA spectrum at 3T before and after mixing (Fig. 1), and measured its relaxation times. With this knowledge, we can use a method similar to the 3-pt Dixon techniques [3, 4] to separate all three species (water, fat and PMMA). The signal  $S_n$  acquired at echo time  $TE_n$  in a pixel is:

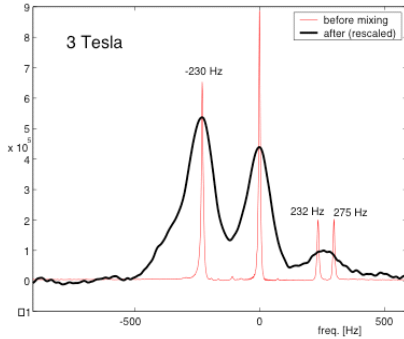


**Figure 1: Spectra obtained at 3T before and after mixing, demonstrating that the location of the spectral peaks do not change after mixing. This data is shown with respect to water.**

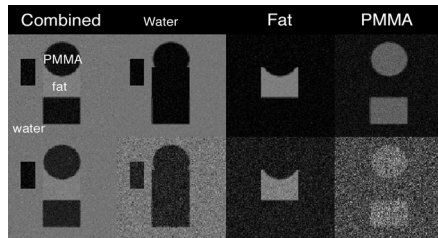


**Figure 3: Simulation demonstrating excellent separation results (top row) when optimal echo times of [13.25, 22.75, 32.25]ms are used. The second row shows poor separation results with suboptimal echo times of [36, 40, 44]ms.**

$$S_n = (\rho_w + \rho_f e^{i2\pi\Delta f_f TE_n} + \rho_p p(TE_n)) e^{i2\pi\psi TE_n} \quad [1]$$

where,  $\rho_w, \rho_f, \rho_p$  are the density of water, fat and PMMA in that pixel,  $\Delta f_f$  is the frequency offset of fat with respect to water,  $\psi$  is the local off-resonance frequency of the pixel, and  $p(t)$  is the signal of PMMA as a function of the echo time (*i.e.*, the Fourier Transform of the PMMA spectrum). As shown in Fig. 1,  $p(t)$  is roughly a sum of four complex exponentials ( $e^{i2\pi\Delta f_i t}$ ). If  $\psi$  is known, the signals  $S_n$  can be demodulated ( $S_n' = S_n / e^{i2\pi\psi TE_n}$ ) and the problem of estimating  $\rho_w, \rho_f, \rho_p$  from signals of three echoes becomes linear and can be written in matrix form:

$$S' = \begin{bmatrix} S_1' \\ S_2' \\ S_3' \end{bmatrix} = \begin{bmatrix} 1 & e^{i2\pi\Delta f_f TE_1} & p(TE_1) \\ 1 & e^{i2\pi\Delta f_f TE_2} & p(TE_2) \\ 1 & e^{i2\pi\Delta f_f TE_3} & p(TE_3) \end{bmatrix} \begin{bmatrix} \rho_w \\ \rho_f \\ \rho_p \end{bmatrix} = \mathbf{A}(\mathbf{TE}) \cdot \boldsymbol{\rho} \quad [2]$$

where  $\boldsymbol{\rho}$  is a vector containing the unknown densities, estimated from  $\mathbf{A}$  and  $S'$ . In general,  $\psi$  is not known. We can acquire a field map  $\psi$  prior to the PMMA injection and use it for the dynamic acquisition. To do this, we will acquire four echoes and use a nonlinear iterative method [4] to determine  $\psi$ . We can optimize the selection of echo delays by developing a cost function that depends on the noise in the images (denoted by  $n$ ). The estimated density of the three materials is given by:

$$\hat{\boldsymbol{\rho}} = \mathbf{A}^{-1}(\mathbf{TE}) \cdot (S' + n) = \boldsymbol{\rho} + \mathbf{A}^{-1}(\mathbf{TE}) \cdot n \quad [3]$$

The term  $\mathbf{A}^{-1}(\mathbf{TE}) \cdot n$  represents the error in the estimated  $\hat{\boldsymbol{\rho}}$ , which is dependent on  $\mathbf{TE}$  (the vector of selected echo times [ $TE_1, TE_2, TE_3$ ]). We formulated a method for choosing  $\mathbf{TE}$  based on the noise performance and other practical considerations. The relative norm error:  $\frac{\|\mathbf{A}^{-1}(\mathbf{TE}) \cdot n\|}{\|n\|}$  is bounded by the condition number of matrix  $\mathbf{A}$ , represented by  $\kappa(\mathbf{A}(\mathbf{TE}))$ , which is the ratio of the maximum and minimum singular values of  $\mathbf{A}$ . An additional consideration is that a short  $\mathbf{TE}$  is also preferred. The optimization problem can be formulated as

$$\text{minimizing: } C(\mathbf{TE}) = \kappa(\mathbf{A}(\mathbf{TE})) + \beta \cdot TE_3 \quad \text{subject to: } \mathbf{TE} \text{ being practically implementable.}$$

Here,  $C(\mathbf{TE})$  is the total cost function,  $TE_3$  is the longest echo time, and  $\beta$  controls any possible tradeoff between optimizing SNR and minimizing  $TE_3$ . The method was evaluated using computer simulations assuming an imaging field strength of 0.5T.

**Results:** Since  $\kappa(\mathbf{A}(\mathbf{TE}))$  is a highly nonlinear function of  $\mathbf{TE}$ , we used a global search to find the minimum  $C(\mathbf{TE})$ . To illustrate the idea, consider the case where the three echoes are equally spaced so there are two degrees of freedom, the first echo time  $TE_1$  and the increment  $\Delta TE$  (this constraint can be easily removed). Fig. 2 shows a plot  $1/C(\mathbf{TE})$  vs.  $TE_1$  and  $\Delta TE$  for  $\beta=0.1$ , a value gives  $\kappa(\mathbf{A}(\mathbf{TE}))$  and  $TE_3$  comparable weight. For this case, the optimal  $\mathbf{TE}$  was [13.25, 22.75, 32.25] ms at 0.5T. The effect of  $\mathbf{TE}$  on the quality of the density estimates was studied with computer simulations. Simulated images had Gaussian noise such that the SNR in water, fat and PMMA in a single image were 10, 11 and 8 respectively. The phantom and its separation with  $\mathbf{TE}=[13.25, 22.75, 32.25]$ ms and a “bad”  $\mathbf{TE}=[36, 40, 44]$ ms are shown in Fig 3. The difference of the separation quality is clearly seen.  $TE_3$ , and therefore the scan time can be shortened by increasing the tradeoff coefficient  $\beta$ . For example, with  $\beta = 0.35$ , the optimal  $\mathbf{TE}$  is [9.75 16.75 23.75] ms.

**Discussion and Conclusion:** MR imaging of PMMA could help monitoring the PMMA injection during a PV procedure. With the modified 3 point Dixon method described above, we should be able to achieve separation of all three materials, which may have application benefits. Alternatively, if echo times  $TE_n$  are selected so that  $e^{i2\pi\Delta f_f TE_n} = 1$ , one is unable to separate fat from water, but can separate PMMA from the other two materials and the system has only three unknowns,  $(\rho_w + \rho_f), \rho_p$ , and  $\psi$ . The general form of  $p(t)$ , in Eq[1] and Eq[2], allows us to include other factors, such as  $T_2$  (or line widths) and relative changes in the amplitudes of the lines with temperature. If the variation of  $p(t)$  with respect to temperature is also known, this method can potentially be extended to determine temperature as well as the amount of materials, which will then require at least a 4-pt acquisition. By including a tradeoff coefficient  $\beta$  in our optimization, we are able to select a set of echo times considering both separated image SNR and short TR constraint. Finally, this multi-point Dixon scheme and echo time selection strategy can be easily extended to other applications, such as imaging of silicone implants.

## Acknowledgement

NIH grants EB00198 and RR09784, the Lucas Foundation and GE Healthcare.

## References

- [1] Zoarski et al. Tech Vasc Interv Radiol. 2002;5(4):223-38. [2] Fahrig et al. Acad Radiol. 2001; 8(12):1200-7.  
[3] Glover et al, JMRI 1991; 1: 521-530. [4] Reeder et al, MRM. 2004;51(1):35-45.

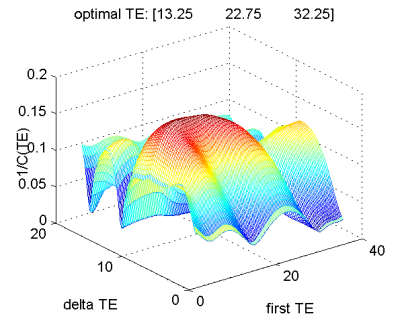


**Figure 2:  $1/C(\mathbf{TE})$  vs. first echo time and  $\Delta TE$  in the case of  $\beta=0.1$ .**